ACS OMEGA

http://pubs.acs.org/journal/acsodf

Article

Synthesis of Ultrastable and Bioconjugable Ag, Au, and Bimetallic Ag_Au Nanoparticles Coated with Calix[4]arenes

Maurice Retout, Ivan Jabin,* and Gilles Bruylants*

Cite This: *ACS Omega* 2021, 6, 19675−19684

Read Online

ACCESS | Metrics & More | Article Recommendations | Supporting Information

ABSTRACT: Compared to gold nanoparticles, silver nanoparticles are largely underexploited for the development of plasmonic nanosensors. This is mainly due to their easy chemical degradation through oxidation, poor colloidal stability, and usually broad size distribution after synthesis, which leads to broad localized surface plasmon resonance bands. Coatings based on polymers such as poly(ethylene glycol) (PEG) or poly(vinylpyrrolidone) (PVP) and plant extracts have been used for the stabilization of AgNPs; however, these thick coatings are not suitable for sensing applications as they isolate the metallic core. The examples of stable AgNPs coated with a thin organic layer remain scarce in comparison to their gold counterparts. In this work, we present a convenient one-step synthesis strategy that allows to obtain unique gold, silver, and bimetallic NPs that combine all of the properties required for biosensing applications. The NPs are stabilized by a tunable calix[4]arene-based monolayer obtained through the reduction of calix[4]arene-tetradiazonium salts. These multidentate ligands are of particular interest as (i) they provide excellent colloidal and chemical stabilities to the particles thanks to their anchoring to the surface via multiple chemical bonds, (ii) they allow the subsequent (bio)conjugation of (bio)molecules under mild conditions, and (iii) they allow a control over the composition of mixed coating layers. Ag and Ag_Au nanoparticles of a high stability are obtained, opening perspectives for development of numerous biosensing applications.

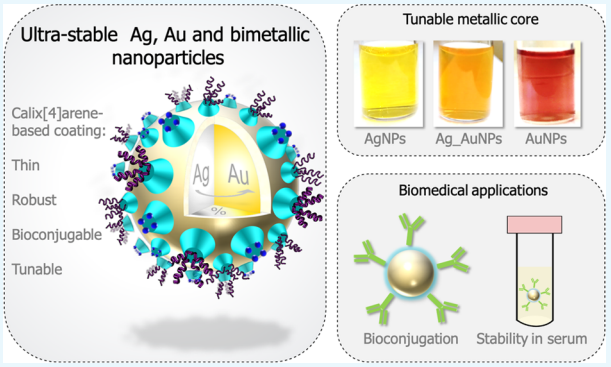

INTRODUCTION

Metal-based nanomaterials can find many applications due to their remarkable catalytic,[1,2] electronic,[3,4] magnetic,[5,6] optical,[7,8] and mechanical[9] properties. These properties depend strongly on the way these nanomaterials are synthesized as it will dictate their final shape, size, composition, and colloidal stability. Gold and silver nanomaterials are extensively studied in the biomedical field thanks to their optical properties.[10−12] Indeed, these nanomaterials exhibit a localized surface plasmon resonance (LSPR) band in the visible region, which strongly depends on their size, shape, and dielectric properties of the local environment.[13,14] Their extinction coefficient is at least three to four orders of magnitude higher than that of any organic molecule.[15,16] Therefore, these nanomaterials constitute attractive transducers for the development of colorimetric biosensors. For now, gold nanoparticles (AuNPs) are the most widely used thanks to their well-mastered synthesis, high chemical stability, and biocompatibility.[17] However, in comparison with AuNPs, AgNPs of the same size exhibit a much higher extinction coefficient and their use could thus greatly improve the biosensor sensitivity.[18] So far, the great potential of silver nanoparticles is underexploited mainly because of their easy chemical degradation through oxidation and their usual poor colloidal stability in the absence of a thick organic coating. In particular, the covalent immobilization of organic molecules at their surface is extremely difficult, as the particles usually aggregate or are degraded upon addition of the functionalization reagents.[17] Consequently, if the synthesis of AgNPs of various sizes is well reported in the presence of citrate as capping agent,[19] their applications in the biosensing field are rather limited[20] and these particles are thus mostly exploited for their antimicrobial properties.[21] Coatings based on polymers such as poly(ethylene glycol) (PEG)[22−24] or poly(vinylpyrrolidone) (PVP)[25] and plant extracts[26,27] have been used for the stabilization of AgNPs (the thinnest coating commercially available is based on a PEG molecule of 3000 Da). These thick coatings are however not suitable for sensing applications as they isolate the metallic core from its environment, which prevents the LSPR band shifts that are usually exploited to detect the presence of an analyte. Moreover, the use of plant extracts leads to AgNPs coated with unknown biomolecules and with nonhomogeneous size

Received: May 4, 2021
Accepted: July 2, 2021
Published: July 19, 2021

https://doi.org/10.1021/acsomega.1c02327
ACS Omega 2021, 6, 19675−19684

Scheme 1. In Situ Synthesis of Calixarene-Coated Silver or Gold Nanoparticles According to the Optimized Procedure[a]

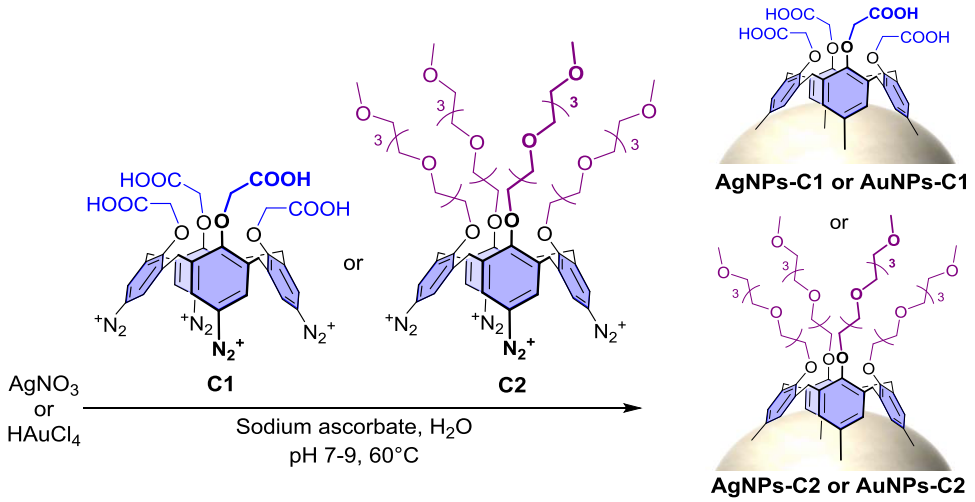

[a]Note that the schematic representation of the grafted calixarenes does not necessarily imply that their four aryl units are linked to the surface.

distribution or shape.[28] In this context, the development of a new method for the synthesis of highly stable AgNPs covered with a thin organic layer that would both provide strong chemical and colloidal stabilities to the particles and allow the covalent immobilization of biomolecules would therefore represent a major breakthrough in the field.

In this work, we report on the use of calix[4]arene-tetradiazonium salt, a preorganized rigid molecular platform decorated with multiple anchoring points,[29−31] as the capping agent. It has indeed already been shown that the reduction of their four aryl diazonium groups into the corresponding aryl radicals leads to their strong and irreversible grafting via the surface multiple links.[32] This method of surface functionalization has been applied with success to a broad range of materials (Au, Ge, carbon, polymers, glass, etc.) over the past decade.[33−36] Moreover, in contrast to what is generally observed with simple aryl diazonium compounds,[37] the unique macrocyclic structure of calix[4]arenes prevents their polymerization at the surface of the material. Thin monolayers of calix[4]arenes are thus typically obtained. Once grafted, the calixarene-based platforms can serve to the covalent immobilization of organic molecules or biomolecules (postfunctionalization step) under mild conditions. This general surface modification strategy has been recently used for the synthesis of robust calixarene-coated AuNPs (AuNPs-calix) through a ligand-exchange procedure from citrate-stabilized AuNPs.[38−40] We thus envisioned that the calix[4]arene-based coating could be a tool of choice for the stabilization of AgNPs. However, as already mentioned, citrate-stabilized AgNP colloids are poorly stable and the particles usually aggregate upon addition of chemicals. In addition, the removal of all of the citrate ligands remains a challenge and the residual citrate molecules at the surface of the nanomaterial may disturb the subsequent postfunctionalization step.[41] For all of these reasons, we investigated the development of a procedure for the in situ synthesis of citrate-free silver or gold NPs by mixing the metallic and calixarene-diazonium salts in the presence of a reducing agent.

Herein, we report on the development of a general procedure for the in situ synthesis of highly stable silver, gold, and bimetallic silver/gold nanoparticles in the presence of calix[4]arene-diazonium salts. The possibility to engineer the composition of the calix[4]arene layer using mixtures of calix[4]arenes and to conjugate organic molecules is also described, opening interesting perspectives in the field of biosensing.

RESULTS AND DISCUSSION

Development of an Optimized Procedure for the In Situ Synthesis of Calixarene-Coated Gold and Silver Nanoparticles. Two calix[4]arene-diazonium salts (i.e., C1 and C2) differing in the nature of their substituents on their small rim were chosen for the study (Scheme 1). Calixarene C1 displays four carboxyl groups on its small rim, that can be used for the subsequent covalent (bio)conjugation of (bio)-molecules, while calixarene C2 bears four PEG chains ended by a methoxy group. It is noteworthy that an attempt to prepare AgNPs-C1 from AgNPs-citrate according to the ligand-exchange procedure that was previously reported on AuNPs-citrate[38−40] led, unsurprisingly, to an irreversible aggregation of the silver particles when the calix[4]arene-diazonium salt C1 and the reducing agent (i.e., $NaBH_4$) were added to the colloidal suspension.

Various reaction conditions (time, temperature, pH, order of addition of the reactants) and reducing agents were screened for the in situ synthesis of calixarene-capped silver (see Table S1) and gold (see Table S2) nanoparticles and the reactions were monitored by UV−vis spectroscopy. Optimal results were obtained by first mixing gold or silver salts with the calix[4]arene-diazonium salt (C1 or C2) at pH between 7 and 9, then adding sodium ascorbate as the reducing agent, and finally stirring the solutions at 60 °C for 16 h (Scheme 1). The resulting calix[4]arene-coated gold or silver nanoparticles were purified from the unreacted reagents by several centrifugation steps and replacement of the supernatant by pure water. The size homogeneity of the obtained nanoparticles was assessed by characterizing the LSPR band, and the density of the organic coating, by monitoring the stability of the suspensions upon pH variations and KF exposure. It is worth mentioning that the optimal synthesis conditions are found for a narrow range of experimental parameters and that conditions differing slightly from the optimal ones lead to either aggregated, polydisperse, or poorly coated particles. This process must result in a delicate balance between the activation

https://doi.org/10.1021/acsomega.1c02327
ACS Omega 2021, 6, 19675−19684

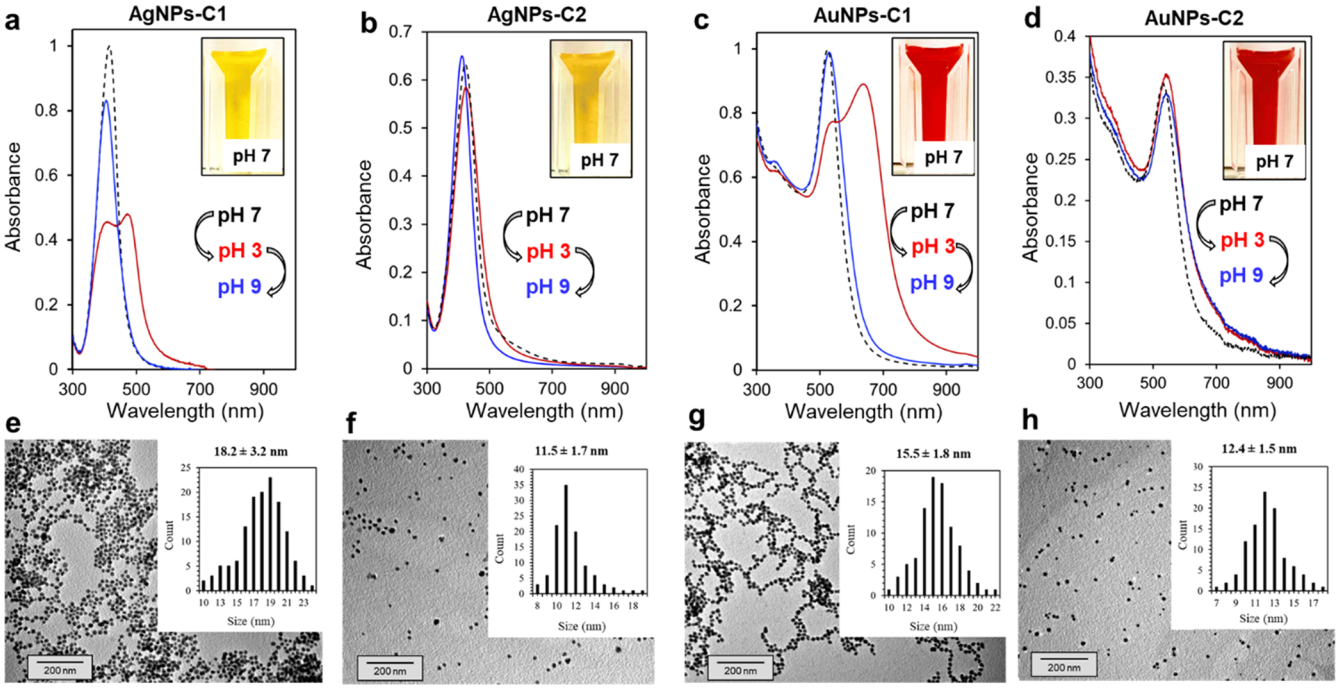

Figure 1. UV−vis spectra of (a) AgNPs-C1, (b) AgNPs-C2, (c) AuNPs-C1, and (d) AuNPs-C2 suspended in water at pH 7 (black dashed line), pH 3 (red plain line), and pH 9 (plain blue line). Insets show pictures of the suspensions at pH 7. TEM images of (e) AgNPs-C1, (f) AgNPs-C2, (g) AuNPs-C1, and (h) AuNPs-C2 with corresponding histograms based on the measurement of >100 NPs.

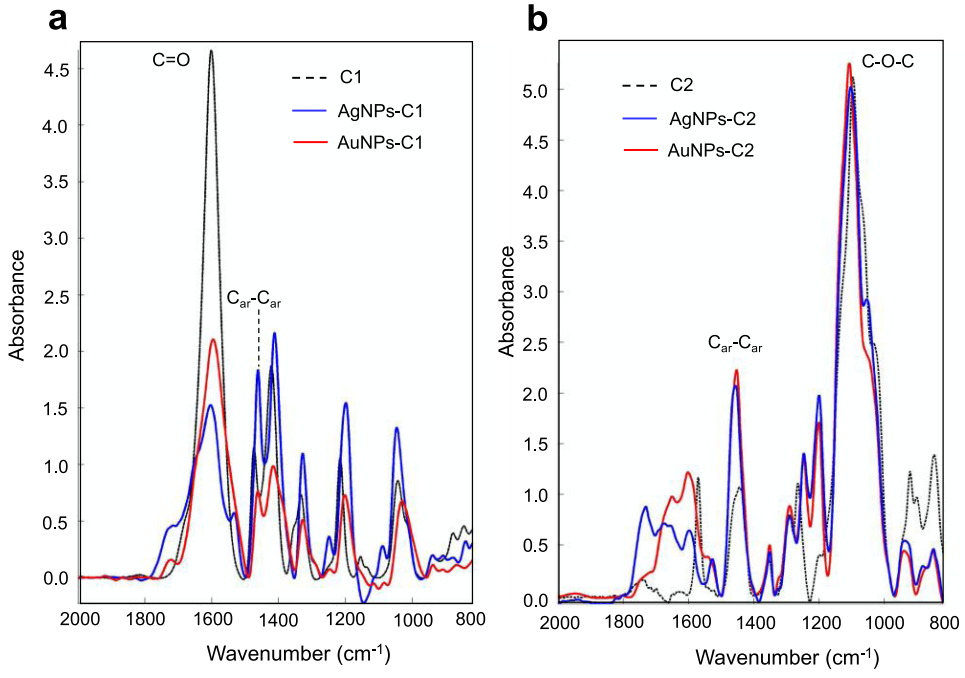

Figure 2. Attenuated total reflection Fourier transform infrared (ATR-FTIR) spectra of (a) calixarene C1, AgNPs-C1, and AuNPs-C1 and (b) calixarene C2, AgNPs-C2, and AuNPs-C2.

of the diazonium groups, reduction of the metallic salts, formation of the metallic cores, grafting of the calixarenes on the NP surface, and their polymerization in solution. The interplay between these different processes and the influence of each parameter (pH, T, or concentrations of different reactants) on several of them leads to a complex synthesis for which only a narrow range of parameters provide monodispersed and well-coated particles. Detailed synthetic and cleaning procedures of the particles can be found in the Experimental Section.

Characterization of NPs-C1 and NPs-C2. AuNPs and AgNPs synthesized in the presence of either C1 (AuNPs-C1 and AgNPs-C1) or C2 (AuNPs-C2 and AgNPs-C2) were characterized by UV−vis and infrared (IR) spectroscopies as well as transmission electron microscopy (TEM) and dynamic light scattering (DLS).

https://doi.org/10.1021/acsomega.1c02327
ACS Omega 2021, 6, 19675−19684

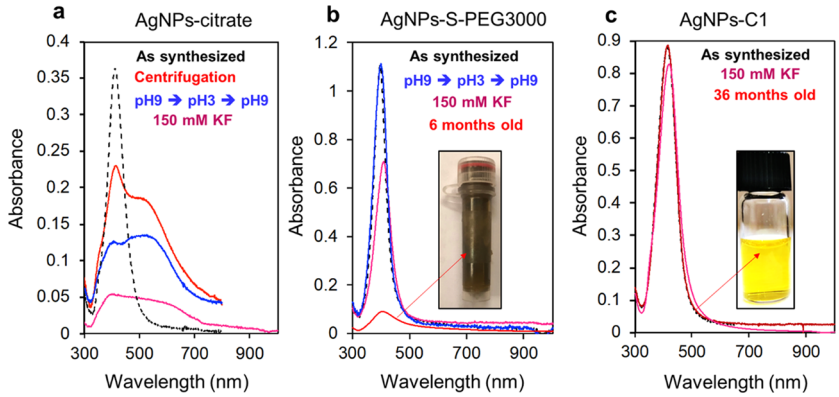

Figure 3. (a) UV−vis spectra of AgNPs-citrate suspended in water (black) after two centrifugation cycles (red), after exposure to pH 3 and then 9 (blue), or after exposure to 150 mM KF for 30 min (pink). (b) UV−vis spectra of AgNPs-S-PEG3000 suspended in water (black) after exposure to pH 3 and then 9 (blue), exposure to 150 mM KF for 30 min (pink), or after 6 months (red). The inset shows a picture of the sample containing 6-month-old AgNPS-S-PEG3000. (c) UV−vis spectra of AgNPs-C1 after exposure to 150 mM KF for 30 min (pink) and after 36 months. Inset shows a picture of the sample containing 36-month-old AgNPS-C1.

The UV−vis spectra of AgNPs-C1, AgNPs-C2, AuNPs-C1, and AuNPs-C2 showed a sharp and intense LSPR band with a maximum of absorbance at 418, 421, 525, and 538 nm, respectively (Figure 1a−d), with resulting suspensions displaying a bright yellow (AgNPs) or deep red (AuNPs) color (Figure 1, insets). The colloidal stability of AgNPs-C1 and AuNPs-C1 is due to the electrostatic repulsion between particles because of the carboxylate groups at their surface; the protonation of these groups in acidic conditions led to an aggregation of the particles and thus to a strong modification of their LSPR bands (Figure 1a,c, spectra in red). However, this aggregation is fully reversible. Indeed, both sets of particles can be fully redispersed by increasing the pH, as shown by the restoration of their LSPR band to their initial wavelengths (Figure 1a,c, spectra in blue). In contrast, AgNPs-C2 and AuNPs-C2 are sterically stabilized thanks to the dense and thicker PEG coating, and are thus not sensitive to pH variations (Figure 1b,d, spectra in red and blue). TEM analysis of the particles revealed a spherical shape and core sizes of 18 ± 3 and 15 ± 2 nm for AgNPs-C1 and AuNPs-C1, respectively. Smaller core sizes of 11 ± 2 and 12 ± 2 nm were observed for AgNPs-C2 and AuNPs-C2, respectively (Figure 1e−h). Additional TEM images of AgNPs-C1 and AuNPs-C1 can be found in the Supporting Information Figures S1 and S2. IR analyses of the particles confirmed the presence of the calix[4]arene-based coating, as the typical bands of C1 (C═O stretching around 1600 cm^{-1}) or C2 (asymmetric C−O−C stretching from the PEG chains around 1100 cm^{-1}) could be observed in NPs-C1 and NPs-C2 spectra, respectively (Figure 2), in addition to the C_{ar}−C_{ar} stretching band that is present at 1458 cm^{-1} in all batches. DLS measurements revealed average hydrodynamic diameters of 37 and 32 nm for AgNPs-C1 and AuNPs-C1, respectively, which correspond to a thin layer around the particles (Figure S3). Hydrodynamic diameters of 46 and 50 nm were measured for AuNPs-C2 and AgNPs-C2 (Figure S4), respectively. These values are in good agreement with those previously reported for a monolayer of C1 or C2 grafted through a ligand-exchange process onto 20 nm citrate-capped AuNPs.[39,40]

It is worth mentioning that using a stronger reducing agent than sodium ascorbate, such as sodium borohydride ($NaBH_4$), allows the synthesis of smaller nanoparticles (i.e., approximately 6 ± 2 nm). As an example, TEM images as well as UV−vis and IR spectra of 6 nm AgNPs-C1 can be seen in Figures S5 and S6, respectively.

Stability and Handling of Calixarene-Coated Silver Nanoparticles. As mentioned above, the use of silver nanoparticles for the development of biosensors is highly challenging because of their very low stability. The silver nanoparticles synthesized in this study were expected to possess higher chemical and colloidal stabilities than the commonly commercially available ones thanks to the multidentate calix[4]arene coating. The stability of the calix[4]arene-coated AgNPs was evaluated and compared with two types of standard commercial AgNPs of similar size (i.e., 20 nm): citrate-capped silver nanoparticles (AgNPs-citrate) and silver nanoparticles coated with a thiolated PEG (3000 Da) (AgNPs-S-PEG3000).

Figure 3 shows the LSPR bands of AgNPs-citrate, AgNPs-S-PEG3000, and AgNPs-C1 after several stability tests. As reported in the literature, AgNPs-citrate are poorly stable. They cannot be centrifuged or exposed to pH variations or agents such as potassium fluoride (KF) without aggregating or degrading almost instantaneously (Figure 3a). In contrast, AgNPs-S-PEG3000 can be centrifuged or exposed to pH variations without any loss of particles or variations of their LSPR band thanks to the thick PEG coating that protects the particles (Figure 3b). However, when exposed to KF for 30 min, a loss of approximately 40% of the particles was observed, indicating that the PEG layer does not efficiently protect the metallic core from the action of fluoride. This moderate stabilization ensured by the thick PEG coating has dramatic consequences on the particle lifetime. After 6 months of storage at 4 °C in the dark, 90% of the particles indeed stuck to the wall of the vial, while the remaining 10% in solution was aggregated. As mentioned previously, calix[4]arene-coated silver nanoparticles AgNPs-C1 and AgNPs-C2 can endure multiple pH variations without degradation (Figure 1). They can also resist to numerous centrifugation cycles without any loss of particles or modification of their LSPR band. When exposed to KF, only a loss of 5% of the particles was observed after 30 min (Figure 3c). Exposure to an oxidizing agent, H_2O_2, has also been investigated. It has been observed that 1.5 × 10^{-3}% of H_2O_2 completely dissolves AgNPs-citrate, while even 3 × 10^{-2}% dissolves only 50% of AgNPs-C1 (see Figure S7).

https://doi.org/10.1021/acsomega.1c02327
ACS Omega 2021, 6, 19675−19684

All of these data indicate that the silver core is remarkably protected from chemical stresses thanks to the calix[4]arene layer. This high stability was illustrated by their extremely long lifetime as no variation of the LSPR band could be observed after 36 months of storage on the bench and in pure water (no reducing or stabilizing agent was added to the suspension). Such a high stability of calix[4]arene-coated AgNPs allows to handle them under conditions that are crucial for the development of biosensing applications. As an example, it is possible to suspend AgNPs-C1 in human serum for 1 h without noticeable loss of particles (Figure 4a), which is not possible with the other AgNPs tested (see Figure S8). It is particularly interesting for in vitro diagnosis, as these kinds of applications require the detection of analytes directly in biological samples. Even more remarkably, it is also possible to dry AgNPs-C2 and resuspend them without any loss (Figure 4b). Finally, the carboxyl groups carried by AgNPs-C1 were used for the covalent immobilization of amino-containing molecules through a peptide coupling reaction. As a proof of concept, an amino-PEG derivative (i.e., H_2N-PEG-OCH_3, see the structure in Figure 4c) was conjugated to AgNPs-C1 via a classical 1-ethyl-3-(3-dimethylaminopropyl)carbodiimide (EDC)/sulfo-NHS procedure, leading to AgNPs-C1-PEG-OCH_3 particles. The choice of this PEG derivative was motivated by the characteristic and distinct IR signals that it possesses compared to AgNPs-C1. Figure 4c shows the IR spectra before and after the coupling reaction (the spectra were normalized on the aromatic band at 1458 cm^{-1}). The typical band of the PEG chain at ca. 1100 cm^{-1} can clearly be identified, confirming the presence of the PEG derivative onto the particles. Furthermore, amide-I and -II bands at ca. 1650 and 1530 cm^{-1}, respectively, were observed, indicating the formation of amide bonds. Finally, the bioconjugation of biomolecules such as peptides or proteins to AgNPs-C1 was also shown through covalent immobilization of a human antibody via the EDC/sulfo-NHS procedure. The presence of the antibody at the surface of the nanoparticles was clearly observed by typical IR amide-I and -II bands at ca. 1650 and 1530 cm^{-1}, respectively (Figure S9). This result highlights the remarkable properties of the calixarene-coated AgNPs and constitutes a significant result in the field of silver nanomaterials for biosensing applications.

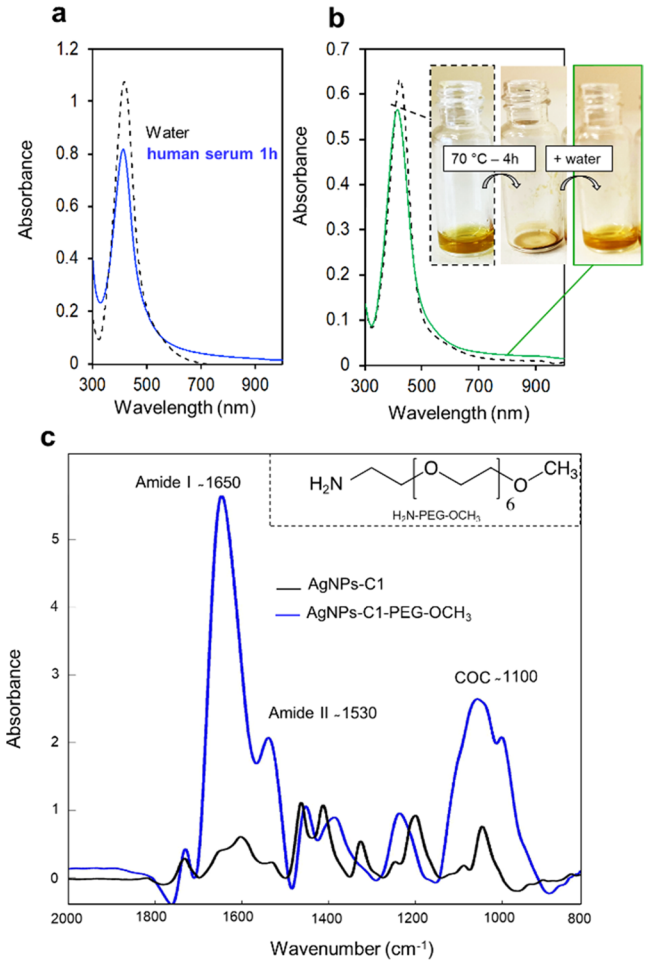

Figure 4. (a) UV−vis spectra of AgNPs-C1 suspended in water (black) or in human serum for 1 h (blue), then centrifuged and resuspended in water. This centrifugation/resuspension step was necessary due to the large absorbance of human serum between 300 and 500 nm. (b) UV−vis spectra of AgNPs-C1 suspended in water before (black) and after drying at 70 °C for 4 h and resuspended in pure water (green). Inset shows pictures of the AgNPs-C1 before drying, after drying, and then resuspended. (c) ATR-FTIR spectra of AgNPs-C1 before (black) and after (blue) conjugation of H_2N-PEG-OCH_3.

Control over the Composition of Calixarene-Based Mixed Layers. For biosensing applications, control over the composition of mixed monolayers of ligands is essential. Particularly, biosensors based on the aggregation of NPs for the detection of biomolecules will operate in the adequate dynamic range only if the number of recognition elements matches the analyte concentration.[42,43] We thus evaluated the possibility to control the formation of mixed layers of calixarenes C1 and C2 on silver and gold nanoparticles. Several batches of particles were synthesized according to the optimized procedure (vide supra) in the presence of different proportions of C1 and C2 (Figure 5a) and the resulting particles AgNPs-C1/C2 or AuNPs-C1/C2 were characterized by IR spectroscopy (Figures S10 and S11). In all cases, the absorbance intensities at 1600 cm^{-1} (C═O band typical of C1) and 1100 cm^{-1} (C−O−C band typical of C2) were compared to determine the composition of the mixed layer at the NP surface. A linear relationship between the ratio of the IR absorbance at 1600 and 1100 cm^{-1}, indicative of the composition of the calixarene coating, and the molar ratio of C1 (%) used during the synthesis was observed (Figure 5b). As NPs-C1 are very sensitive to pH variations, unlike NPs-C2 (vide supra), the pH sensitivity of NPs-C1/C2 was thus studied by UV−vis spectroscopy to evaluate the proportion of the two calixarenes at the surface (Figures S12 and S13). Figure 5c shows the LSPR shift of the different NP-C1/C2 batches when decreasing the pH from 7 to 3 as a function of the molar ratio of C1 (%) used during the NP synthesis. A proportional relationship between the λ_{max} shift and the percentage of C1 can be observed. All of these data clearly show that the composition of the calixarene-based coating is directly proportional to the proportions of C1 and C2 used during the nanoparticle synthesis. This finding is of great interest as it means that it is possible to simply tune the surface properties of the NPs as well as their bioconjugation capacity. Indeed, increasing the proportion of C2 at the surface leads to sterically stabilized NPs thanks to the increased density of PEG chains, while increasing the proportion of C1 leads to a higher density in bioconjugable carboxylate groups at the NP surface.

https://doi.org/10.1021/acsomega.1c02327
ACS Omega 2021, 6, 19675−19684

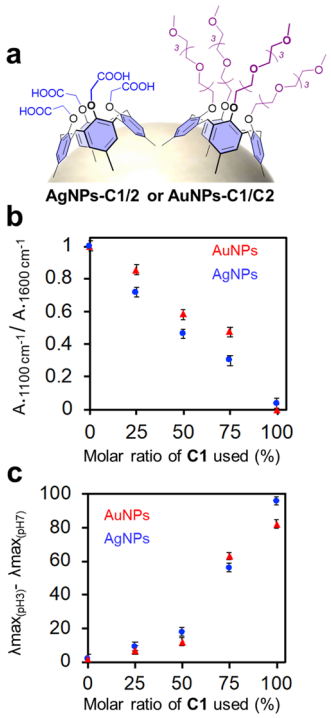

Figure 5. (a) Scheme of Ag- or AuNPs coated by a mixed layer of calixarenes C1 and C2. (b) Normalized ratio of the IR absorbance at 1100 and 1600 cm^{-1} of AgNPs-C1/C2 (blue) and AuNPs-C1/C2 (red) as a function of the molar ratio of C1 (%) used during the synthesis. (c) Difference between the maximum of absorbance at pH 3 and 7 of AgNPs-C1/C2 (blue) and AuNPs-C1/C2 (red) as a function of the molar ratio of C1 (%) used during the synthesis.

Control over the Optical Properties. The last challenge was to produce bimetallic calixarene-coated nanoparticles. This kind of particle shows great promise for biomedical imaging and sensing or in catalysis as they offer a new degree of freedom to tune the particle properties and combine the advantages of both metals in a single nanostructure.[44,45] Coprecipitation of Ag and Au has already been reported in the literature to produce alloyed nanoparticles with a global composition matching that of the salt mixture used for the preparation of the particles, although the distribution of the two metals in the NP is not uniform.[45] Several batches of nanoparticles were synthesized in the presence of a mixture of silver and gold salts mixed with either C1 (Ag_AuNPs-C1) or C2 (Ag_AuNPs-C2) according to the optimized procedure (vide supra). Different molar ratios of silver and gold salts were used, and the resulting suspensions were characterized by UV−vis spectroscopy (Figure 6c,d). For all of the samples, a strong and sharp LSPR band was observed with a maximum of absorbance ranging from the one of pure silver nanoparticles to that of pure gold nanoparticles, i.e., suspension colors from bright yellow to bright red (Figure 6a,b). Most interestingly, a linear relationship between the position of LSPR λ_{max} and the proportion of the two metal salts used for the NP synthesis was also observed (Figure 6c,d, insets). This suggests that, as observed by Ristig et al., a control over the global composition of the metallic core can be obtained.[45] TEM images showed that the size and shape of the bimetallic nanoparticles were similar to those of pure gold or silver nanoparticles, i.e., 13 ± 3 nm for alloys coated with C1 and 10 ± 3 nm for alloys coated with C2 (Figures S14 and S15). Finally, all of the samples were characterized by IR spectroscopy and typical bands of calixarenes C1 and C2 were observed on Ag_AuNPs-C1 and Ag_AuNPs-C2, respectively (Figure S16), confirming the presence of the calixarene layer.

Finally, this versatile procedure was extended to the production of bimetallic nanoparticles coated with mixed layers of calix[4]arenes (Figure 7a). These sophisticated NPs possess the optical properties of alloyed particles and colloidal properties that reflect the ratio of C1 and C2 in the grafted

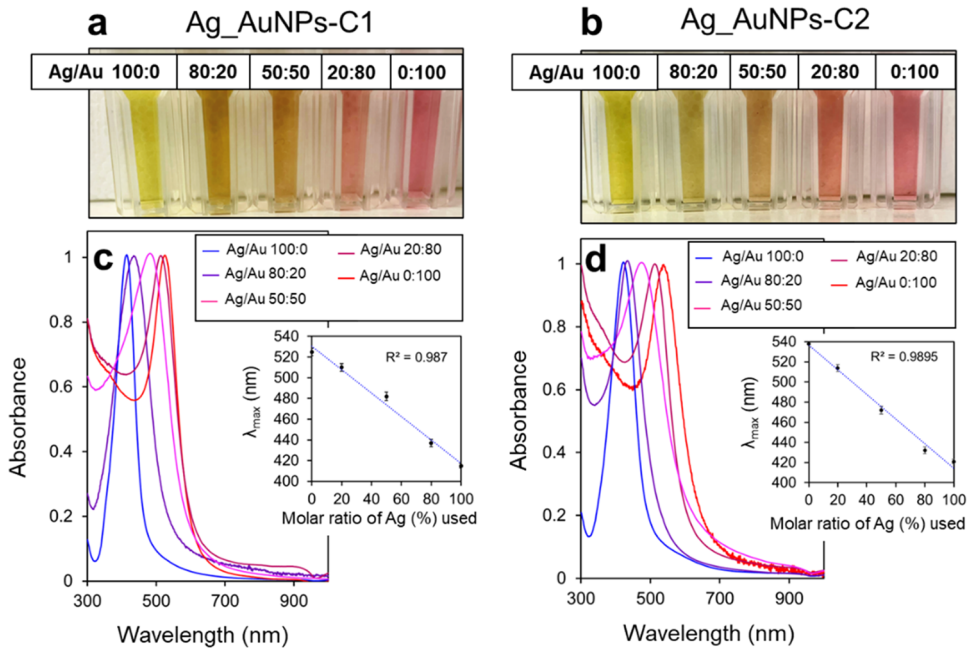

Figure 6. Pictures of suspensions of (a) Ag_AuNPs-C1 and (b) Ag_AuNPs-C2 produced with different molar ratios of $AgNO_3$ (%) and $HAuCl_4$ and (c and d) corresponding normalized UV−vis spectra. Insets show the position of the maximum of absorbance as a function of the molar ratio of $AgNO_3$ (%) used during the synthesis.

https://doi.org/10.1021/acsomega.1c02327
ACS Omega 2021, 6, 19675−19684

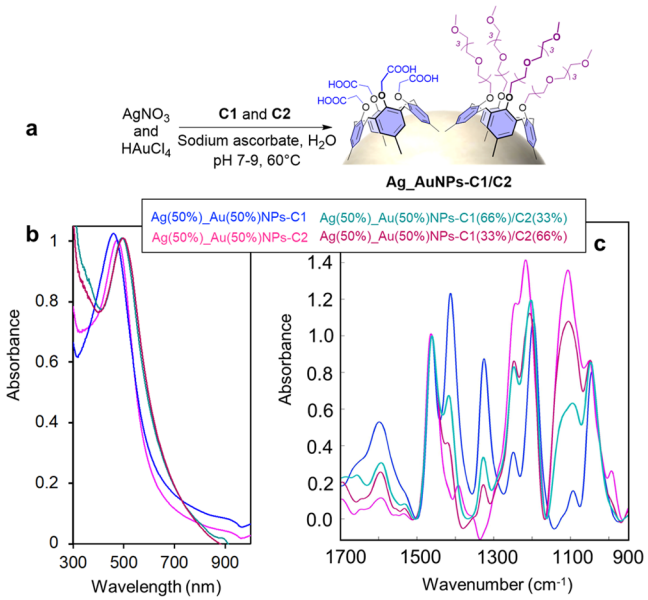

Figure 7. (a) Scheme of the synthesis of bimetallic Ag_Au nanoparticles coated with a mixed layer of calixarenes. (b) UV−vis and (c) ATR-FTIR spectra of bimetallic nanoparticles synthesized in the presence of a mixture of silver and gold salts and a mixture of C1 and C2.

calixarene layer. As an example, equimolar solutions of gold and silver salts were mixed with mixtures of C1 and C2 containing different molar ratios (%) C1/C2 of 100:0, 66:33, 33:66, and 0:100. The resulting Ag(50%)_Au(50%)-C1/C2 particles were characterized by UV−vis, IR, and TEM.

UV−vis spectroscopy revealed a similar absorbance maximum for all of the suspensions (Figure 7b), which was expected, as the composition of the metallic cores was kept constant. IR spectra revealed the obtention of mixed layers of calixarenes with different C1 and C2 proportions on the bimetallic particles as different IR signal intensities of C1 and C2 were observed, as previously described (Figure 7c). Finally, TEM analysis of these particles revealed a spherical shape with a size comprised between that of Ag(50%)_Au(50%)NPs-C1 and Ag(50%)_Au(50%)NPs-C2. As an example, the TEM picture of Ag(50%)_Au(50%)NPs-C1(50%)/C2(50%) is reported in Figure S17 and shows a core size of 13 ± 2 nm.

These particles represent an important step toward the development of biomedical applications, as both their optical properties and organic coating can be precisely tuned using this simple one-pot synthesis procedure. As both the calixarene-coated pure AgNPs and AuNPs present excellent stabilities and a tunable bioconjugation capacity depending on the proportion of C1 in the organic layer, those alloyed NPs are expected to be characterized by similar properties.

CONCLUSIONS

Herein, we report a versatile and very simple in situ synthesis method to produce ultrastable Ag, Au, or Ag_Au nanoparticles. All of these NPs are coated by a thin layer of calix[4]arenes. These molecular platforms are of particular interest as NP coating ligands, since they provide (i) high colloidal and chemical stabilities despite the thinness of the organic layer and (ii) a bioconjugation capacity. Furthermore, they can be functionalized at the level of their small rim with a large variety of functional groups without affecting the reactivity of the diazonium groups at their large rim (and the subsequent grafting to the surface), allowing the grafting of mixed layers on the NPs. With this NP synthesis method, mixed layers of C1 and C2 and/or Ag_Au bimetallic nanoparticles could be obtained by tuning the proportions of C1 and C2 or of silver and gold salts, respectively, before addition of the reducing agent. Therefore, it is possible to control the composition of the calix[4]arene layer (and thus the surface properties of the particles) as well as the optical properties of the particles, paving the way for the synthesis of highly tunable ultrastable gold, silver, and alloyed nanoparticles.

We then show that silver nanoparticles produced with this synthesis possess a very high chemical stability despite the thinness of the organic coating. Their stability encompasses by far the one of the commercially available AgNPs, allowing their use in human serum, drying, or covalent (bio)conjugation with amine-containing (bio)molecules via a classical EDC/sulfo-NHS procedure. We think that this method is of general interest in the field of metallic nanoparticle synthesis. Indeed, highly stable nanoparticles coated with a thin engineered organic layer are obtained in a simple one-step synthetic procedure with (i) a control over the composition of the organic coating and (ii) with tunable optical properties. It could significantly improve the development of biosensors based on the use of plasmonic nanoparticles, especially composed of silver. Efforts are ongoing to extend this synthesis process to nanoparticles of other metals such as copper, palladium, platinum, or even to magnetic nanoparticles.

EXPERIMENTAL SECTION

General Materials. Tetrachloroauric(III) acid ($HAuCl_4$) and sodium ascorbate citrate ($C_6H_7NaO_6$) were purchased from Sigma-Aldrich (Saint-Louis, MO). Silver nitrate was purchased from VWR Chemical (Radnor, Pennsylvania). All solutions were prepared with HPLC-grade water (Lichrosolv) and all reagent solutions were aqueous unless otherwise noted. Calix[4]arenes C1 and C2 were purchased from X4C (Belgium). Before use, all glassware and Teflon-coated stir bars were washed with aqua regia (3:1 volume ratio of concentrated HCl and HNO_3) and rinsed thoroughly with water.

Caution! Although we have not encountered any problem, it is noted that diazonium salt derivatives are potentially explosive and should be handled with appropriate precautions. Aqua regia is highly toxic and corrosive and requires proper personal protective equipment. Aqua regia should only be handled in a fume hood.

Nanoparticle Synthesis. Typically, 150 μL of an aqueous solution of $AgNO_3$ (10 mM) or $HAuCl_4$ (10 mM) or a mixture of both were mixed with 575 μL of lichrosolv water and 360 μL of an aqueous solution of C1 (5 mM) or C2 (5 mM) or a mixture of both. As an example, Ag(50%)_Au(50%)NPs were synthesized using a mixture solution containing 75 μL of the aqueous solution of $AgNO_3$ (10 mM) and 75 μL of the aqueous solution of $HAuCl_4$ (10 mM). NPs-C1(50%)/C2(50%) were synthesized using a solution obtained by mixing 180 μL of the aqueous solution of C1 (5 mM) and 180 μL of the aqueous solution of C2 (5 mM). The pH was increased to a value comprised between 7 and 9 through the addition of an appropriate volume of 1 M NaOH (typically between 10 and 20 μL depending on the metal salt or the calix[4]arene used). Quickly after this, 410 μL of an aqueous solution of sodium ascorbate (15 mM) was added and

https://doi.org/10.1021/acsomega.1c02327
ACS Omega 2021, 6, 19675−19684

the resulting solution was stirred for 16 h at 60 °C. After ca. 10 min, a change of color of the solution can be clearly observed, becoming yellow for AgNPs, red for AuNPs, and orange for Ag_AuNPs. At the end of the reaction, the nanoparticles were washed by centrifugation. Briefly, the NPs were centrifuged at 20 000*g* for 20 min, and the supernatant was removed and replaced by 5 mM NaOH or 1% SDS (mass) for particles synthesized in the presence of calix[4]arenes C1 or C2, respectively. In the case of the mixture of C1 and C2, 1% SDS was also used. This process was repeated two times, then two other cycles were performed with replacement of the supernatant by pure water. Four cycles were then performed to completely discard all of the unreacted reagents as well as small and noncoated particles. It is worth to mention that the first supernatant was colored due to the presence of small particles that do not precipitate at this centrifugation force. The concentration of AuNPs or AgNPs was determined by measuring their diameter by TEM and recording their absorption spectra, using the extinction coefficients of 8×10^8 or 6×10^9 $L \cdot cm^{-1} \cdot mol^{-1}$, respectively, reported in the literature for particles of these sizes.[15,16]

Conjugation of NPs-C1. Nanoparticles were diluted in MES buffer (20 mM, pH 5.5) to reach a nanoparticle concentration of 1 nM in a volume of 300 μL. To this dispersion, 20 μL of an aqueous solution of 1-ethyl-3-(3-dimethylaminopropyl)carbodiimide (EDC, 6 mM) and 20 μL of an aqueous solution of *N*-hydroxysulfosuccinimide (sulfo-NHS, 10 mM) were added. The resulting solution was stirred at room temperature for 1 h to activate the carboxyl groups carried by the NPs. After 1 h, 1 mL of pure water was added, and the particles were centrifuged at 20 000*g* for 20 min. The supernatant was then discarded and replaced by 450 μL of pure water. Ultrasonication was used when necessary to resuspend the particles. Finally, an appropriate volume of molecules containing an amino group was added to reach 10 000 equiv per particle and the solution was stirred for 4 h at room temperature. The particles were then cleaned from the excess of reagent and adsorbed molecules via centrifugation cycles: two cycles involving replacement of the supernatant with 1% SDS in mass to ensure the removal of adsorbed molecules followed by two cycles with pure water to remove the SDS.

UV−Vis Spectroscopy. UV−vis absorption spectra were recorded from 1000 to 300 nm at a 120 $nm \cdot min^{-1}$ scan speed with a UV−vis−NIR spectrophotometer in disposable (poly(methyl methacrylate), PMMA) cuvettes with a 1 cm optical path length at room temperature.

Dynamic Light Scattering. Samples were characterized by dynamic light scattering (DLS) with back scattering (NIBS 173°). Measurements were performed at 25 °C using a refractive index of 1.54 for the gold nanoparticles. AuNPs (20 μL, ∼16 nM) were dispersed in lichrosolv water to obtain 1 mL of AuNPs (∼0.16 nM) in disposable semi-microcuvettes (PMMA) and multiple DLS measurements were performed. The reported values are the average hydrodynamic diameters obtained from three independent measurements using the *Z* average as calculated by the Zetasizer software.

Attenuated Total Reflection Fourier Transform Infrared. Attenuated total reflection Fourier transform infrared (ATR-FTIR) spectra were recorded at 22 °C on an FTIR spectrophotometer equipped with a liquid-nitrogen-cooled mercury−cadmium−telluride detector. The spectrophotometer was continuously purged with dried air. The target chemicals were deposited in solution on a germanium single-crystal internal reflection element (triangular prism of 6.8 mm × 45 mm, with an internal incidence angle of 45°), and the solvent was removed with a flow of nitrogen gas. Bare germanium was used for the background spectrum. Opus software (4.2.37) was used to record 128 scans with a nominal resolution of 2 cm^{-1}. Data were processed and analyzed using the home written Kinetics package in Matlab R2013a by subtraction of water vapor, baseline correction, and apodization at 10 cm^{-1}.

Transmission Electron Microscopy. Images of the AuNPs were obtained with a Philips CM20-UltraTWIN transmission electron microscope (TEM) equipped with a lanthanum hexaboride (LaB6) crystal at a 200 kV accelerating voltage. The average size and 95% confidence interval were determined by measuring the size of more than 100 AuNPs.

■ ASSOCIATED CONTENT

Supporting Information

The Supporting Information is available free of charge at https://pubs.acs.org/doi/10.1021/acsomega.1c02327.

DLS of NPs-C1; UV−vis, IR, and TEM of 6 nm AgNPs-C1; UV−vis and IR of NPs-C1/C2; IR and TEM images of Ag_AuNPs; and TEM images of Ag(50%)_Au(50%)-NPs-C1(50%)/C2(50%) (PDF)

■ AUTHOR INFORMATION

Corresponding Authors

Ivan Jabin − *Laboratoire de Chimie Organique, Université libre de Bruxelles (ULB), B-1050 Brussels, Belgium;* orcid.org/0000-0003-2493-2497; Email: Ivan.Jabin@ulb.be

Gilles Bruylants − *Engineering of Molecular NanoSystems, Ecole Polytechnique de Bruxelles, Université libre de Bruxelles (ULB), B-1050 Brussels, Belgium;* orcid.org/0000-0003-1752-5826; Email: Gilles.Bruylants@ulb.be

Author

Maurice Retout − *Engineering of Molecular NanoSystems, Ecole Polytechnique de Bruxelles, Université libre de Bruxelles (ULB), B-1050 Brussels, Belgium*

Complete contact information is available at: https://pubs.acs.org/10.1021/acsomega.1c02327

Notes

The authors declare no competing financial interest.

■ ACKNOWLEDGMENTS

The "Actions de Recherches Concertées" of the Fédération Wallonie-Bruxelles and the ULB (Ph.D. grant to M.R.) are acknowledged for financial support.

■ REFERENCES

(1) Trzeciak, A. M.; Augustyniak, A. W. The Role of Palladium Nanoparticles in Catalytic C−C Cross-Coupling Reactions. *Coord. Chem. Rev.* **2019**, *384*, 1−20.

(2) Bai, L.; Wang, X.; Chen, Q.; Ye, Y.; Zheng, H.; Guo, J.; Yin, Y.; Gao, C. Explaining the Size Dependence in Platinum-Nanoparticle-Catalyzed Hydrogenation Reactions. *Angew. Chem., Int. Ed.* **2016**, *55*, 15656−15661.

(3) Kefeni, K. K.; Msagati, T. A. M.; Mamba, B. B. Ferrite Nanoparticles: Synthesis, Characterisation and Applications in Electronic Device. *Mater. Sci. Eng., B.* **2017**, *215*, 37−55.

(4) Zhu, W.; Wu, Z.; Foo, G. S.; Gao, X.; Zhou, M.; Liu, B.; Veith, G. M.; Wu, P.; Browning, K. L.; Lee, H. N.; Li, H.; Dai, S.; Zhu, H. Taming Interfacial Electronic Properties of Platinum Nanoparticles on Vacancy-Abundant Boron Nitride Nanosheets for Enhanced Catalysis. *Nat. Commun.* **2017**, *8*, No. 15291.
(5) Hedayatnasab, Z.; Abnisa, F.; Daud, W. M. A. W. Review on Magnetic Nanoparticles for Magnetic Nanofluid Hyperthermia Application. *Mater. Des.* **2017**, *123*, 174−196.
(6) Gloag, L.; Mehdipour, M.; Chen, D.; Tilley, R. D.; Gooding, J. J. Advances in the Application of Magnetic Nanoparticles for Sensing. *Adv. Mater.* **2019**, *31*, No. 1904385.
(7) Wu, Y.; Ali, M. R. K.; Chen, K.; Fang, N.; El-Sayed, M. A. Gold Nanoparticles in Biological Optical Imaging. *Nano Today* **2019**, *24*, 120−140.
(8) Sharifi, M.; Attar, F.; Saboury, A. A.; Akhtari, K.; Hooshmand, N.; Hasan, A.; El-Sayed, M. A.; Falahati, M. Plasmonic Gold Nanoparticles: Optical Manipulation, Imaging, Drug Delivery and Therapy. *J. Control. Release* **2019**, *311−312*, 170−189.
(9) Chen, Y.; Zheng, K.; Niu, L.; Zhang, Y.; Liu, Y.; Wang, C.; Chu, F. Highly Mechanical Properties Nanocomposite Hydrogels with Biorenewable Lignin Nanoparticles. *Int. J. Biol. Macromol.* **2019**, *128*, 414−420.
(10) Jain, P. K.; Huang, X.; El-Sayed, I. H.; El-Sayed, M. A. Review of Some Interesting Surface Plasmon Resonance-Enhanced Properties of Noble Metal Nanoparticles and Their Applications to Biosystems. *Plasmonics* **2007**, *2*, 107−118.
(11) Khlebtsov, N. G.; Dykman, L. A. Optical Properties and Biomedical Applications of Plasmonic Nanoparticles. *J. Quant. Spectrosc. Radiat. Transf.* **2010**, *111*, 1−35.
(12) Park, J.-E.; Kim, M.; Hwang, J.-H.; Nam, J.-M. Golden Opportunities: Plasmonic Gold Nanostructures for Biomedical Applications Based on the Second Near-Infrared Window. *Small Methods* **2017**, No. 1600032.
(13) Kelly, K. L.; Coronado, E.; Zhao, L. L.; Schatz, G. C. The Optical Properties of Metal Nanoparticles: The Influence of Size, Shape, and Dielectric Environment. *J. Phys. Chem. B* **2003**, *107*, 668−677.
(14) Link, S.; El-Sayed, M. A. Spectral Properties and Relaxation Dynamics of Surface Plasmon Electronic Oscillations in Gold and Silver Nanodots and Nanorods. *J. Phys. Chem. B* **1999**, *103*, 8410−8426.
(15) Liu, X.; Atwater, M.; Wang, J.; Huo, Q. Extinction Coefficient of Gold Nanoparticles with Different Sizes and Different Capping Ligands. *Colloids Surfaces B Biointerfaces* **2007**, *58*, 3−7.
(16) Paramelle, D.; Sadovoy, A.; Gorelik, S.; Free, P.; Hobley, J.; Fernig, D. G. A Rapid Method to Estimate the Concentration of Citrate Capped Silver Nanoparticles from UV-Visible Light Spectra. *Analyst* **2014**, *139*, 4855−4861.
(17) Huang, X.; Liu, Y.; Yung, B.; Xiong, Y.; Chen, X. Nanotechnology-Enhanced No-Wash Biosensors for in Vitro Diagnostics of Cancer. *ACS Nano* **2017**, *11*, 5238−5292.
(18) Thompson, D. G.; Enright, A.; Faulds, K.; Smith, W. E.; Graham, D. Ultrasensitive DNA Detection Using Oligonucleotide-Silver Nanoparticle Conjugates. *Anal. Chem.* **2008**, *80*, 2805−2810.
(19) Bastús, N. G.; Merkoçi, F.; Piella, J.; Puntes, V. Synthesis of Highly Monodisperse Citrate-Stabilized Silver Nanoparticles of up to 200 Nm: Kinetic Control and Catalytic Properties. *Chem. Mater.* **2014**, *26*, 2836−2846.
(20) Pinzaru, I.; Coricovac, D.; Dehelean, C.; Moacă, E. A.; Mioc, M.; Baderca, F.; Sizemore, I.; Brittle, S.; Marti, D.; Calina, C. D.; Tsatsakis, A. M.; Şoica, C. Stable PEG-Coated Silver Nanoparticles − A Comprehensive Toxicological Profile. *Food Chem. Toxicol.* **2018**, *111*, 546−556.
(21) Senjen, R. *Nano and Biocidal Silver: Extreme Germ Killers Present a Growing Threat to Public Health*; Friends of Earth, June 2009; pp 1−47.
(22) Mandal, A.; Meda, V.; Zhang, W. J.; Farhan, K. M.; Gnanamani, A. Synthesis, Characterization and Comparison of Antimicrobial Activity of PEG/TritonX-100 Capped Silver Nanoparticles on Collagen Scaffold. *Colloids Surf., B* **2012**, *90*, 191−196.
(23) Hefni, H. H. H.; Azzam, E. M.; Badr, E. A.; Hussein, M.; Tawfik, S. M. Synthesis, Characterization and Anticorrosion Potentials of Chitosan-g-PEG Assembled on Silver Nanoparticles. *Int. J. Biol. Macromol.* **2016**, *83*, 297−305.
(24) Barbalinardo, M.; Caicci, F.; Cavallini, M.; Gentili, D. Protein Corona Mediated Uptake and Cytotoxicity of Silver Nanoparticles in Mouse Embryonic Fibroblast. *Small* **2018**, *14*, No. 1801219.
(25) Vazquez-Muñoz, R.; Arellano-Jimenez, M. J.; Lopez, F. D.; Lopez-Ribot, J. L. Protocol Optimization for a Fast, Simple and Economical Chemical Reduction Synthesis of Antimicrobial Silver Nanoparticles in Non-Specialized Facilities. *BMC Res. Notes* **2019**, *12*, 1−6.
(26) Von White, G.; Kerscher, P.; Brown, R. M.; Morella, J. D.; McAllister, W.; Dean, D.; Kitchens, C. L. Green Synthesis of Robust, Biocompatible Silver Nanoparticles Using Garlic Extract. *J. Nanomater.* **2012**, *2012*, 1−12.
(27) Gavamukulya, Y.; Maina, E. N.; Meroka, A. M.; Madivoli, E. S.; El-Shemy, H. A.; Wamunyokoli, F.; Magoma, G. Green Synthesis and Characterization of Highly Stable Silver Nanoparticles from Ethanolic Extracts of Fruits of Annona Muricata. *J. Inorg. Organomet. Polym. Mater.* **2020**, *30*, 1231−1242.
(28) Rauwel, P.; Küünal, S.; Ferdov, S.; Rauwel, E. A Review on the Green Synthesis of Silver Nanoparticles and Their Morphologies Studied via TEM. *Adv. Mater. Sci. Eng.* **2015**, *2015*, 1−9.
(29) Ray, P.; Clément, M.; Martini, C.; Abdellah, I.; Beaunier, P.; Rodriguez-Lopez, J. L.; Huc, V.; Remita, H.; Lampre, I. Stabilisation of Small Mono- and Bimetallic Gold-Silver Nanoparticles Using Calix[8]Arene Derivatives. *New J. Chem.* **2018**, *42*, 14128−14137.
(30) Li, Z.-Q.; Tang, J.-H.; Zhong, Y.-W. Multidentate Anchors for Surface Functionalization. *Chem. - An Asian J.* **2019**, *14*, 3119−3126.
(31) Clément, M.; Abdellah, I.; Martini, C.; Fossard, F.; Dragoe, D.; Remita, H.; Huc, V.; Lampre, I. Gold(i)-Silver(i)-Calix[8]Arene Complexes, Precursors of Bimetallic Alloyed Au-Ag Nanoparticles. *Nanoscale Adv.* **2020**, *2*, 2768−2773.
(32) Troian-Gautier, L.; Mattiuzzi, A.; Reinaud, O.; Lagrost, C.; Jabin, I. Use of Calixarenes Bearing Diazonium Groups for the Development of Robust Monolayers with Unique Tailored Properties. *Org. Biomol. Chem.* **2020**, *18*, 3624−3637.
(33) Blond, P.; Mattiuzzi, A.; Valkenier, H.; Troian-Gautier, L.; Bergamini, J. F.; Doneux, T.; Goormaghtigh, E.; Raussens, V.; Jabin, I. Grafting of Oligo(Ethylene Glycol)-Functionalized Calix[4]Arene-Tetradiazonium Salts for Antifouling Germanium and Gold Surfaces. *Langmuir* **2018**, *34*, 6021−6027.
(34) Troian-Gautier, L.; Martínez-Tong, D. E.; Hubert, J.; Reniers, F.; Sferrazza, M.; Mattiuzzi, A.; Lagrost, C.; Jabin, I. Controlled Modification of Polymer Surfaces through Grafting of Calix[4]Arene-Tetradiazoate Salts. *J. Phys. Chem. C* **2016**, *120*, 22936−22945.
(35) Mattiuzzi, A.; Jabin, I.; Mangeney, C.; Roux, C.; Reinaud, O.; Santos, L.; Bergamini, J. F.; Hapiot, P.; Lagrost, C. Electrografting of Calix[4]Arenediazonium Salts to Form Versatile Robust Platforms for Spatially Controlled Surface Functionalization. *Nat. Commun.* **2012**, *3*, No. 1130.
(36) Santos, L.; Mattiuzzi, A.; Jabin, I.; Vandencasteele, N.; Reniers, F.; Reinaud, O.; Hapiot, P.; Lhenry, S.; Leroux, Y.; Lagrost, C. One-Pot Electrografting of Mixed Monolayers with Controlled Composition. *J. Phys. Chem. C* **2014**, *118*, 15919−15928.
(37) Pinson, J.; Podvorica, F. Attachment of Organic Layers to Conductive or Semiconductive Surfaces by Reduction of Diazonium Salts. *Chem. Soc. Rev.* **2005**, *34*, 429−439.
(38) Troian-Gautier, L.; Valkenier, H.; Mattiuzzi, A.; Jabin, I.; Van Den Brande, N.; Van; Mele, B.; Hubert, J.; Reniers, F.; Bruylants, G.; Lagrost, C.; Leroux, Y. Extremely Robust and Post-Functionalizable Gold Nanoparticles Coated with Calix[4]Arenes via Metal-Carbon Bonds. *Chem. Commun.* **2016**, *52*, 10493−10496.
(39) Valkenier, H.; Malytskyi, V.; Blond, P.; Retout, M.; Mattiuzzi, A.; Goole, J.; Raussens, V.; Jabin, I.; Bruylants, G. Controlled Functionalization of Gold Nanoparticles with Mixtures of Calix[4]-

https://doi.org/10.1021/acsomega.1c02327
ACS Omega 2021, 6, 19675−19684

Arenes Revealed by Infrared Spectroscopy. *Langmuir* **2017**, *33*, 8253−8259.
(40) Retout, M.; Blond, P.; Jabin, I.; Bruylants, G. Ultrastable PEGylated Calixarene-Coated Gold Nanoparticles with a Tunable Bioconjugation Density for Biosensing Applications. *Bioconjugate Chem.* **2021**, *32*, 290−300.
(41) Park, J.-W.; Shumaker-Parry, J. S. Strong Resistance of Citrate Anions on Metal Nanoparticles to Desorption under Thiol Functionalization. *ACS Nano* **2015**, *9*, 1665−1682.
(42) Huang, C.-C.; Huang, Y.-F.; Cao, Z.; Tan, W.; Chang, H. T. Aptamer-Modified Gold Nanoparticles for Colorimetric Determination of Platelet-Derived Growth Factors and Their Receptors. *Anal. Chem.* **2005**, *77*, 5735−5741.
(43) He, H.; Feng, M.; Chen, Q.; Zhang, X.; Zhan, H. Light-Induced Reversible Self-Assembly of Gold Nanoparticles Surface-Immobilized with Coumarin Ligands. *Angew. Chem.* **2016**, *128*, 948−952.
(44) Loza, K.; Heggen, M.; Epple, M. Synthesis, Structure, Properties, and Applications of Bimetallic Nanoparticles of Noble Metals. *Adv. Funct. Mater.* **2020**, *30*, No. 1909260.
(45) Ristig, S.; Prymak, O.; Loza, K.; Gocyla, M.; Meyer-Zaika, W.; Heggen, M.; Raabe, D.; Epple, M. Nanostructure of Wet-Chemically Prepared, Polymer-Stabilized Silver-Gold Nanoalloys (6 Nm) over the Entire Composition Range. *J. Mater. Chem. B* **2015**, *3*, 4654−4662.

https://doi.org/10.1021/acsomega.1c02327
ACS Omega 2021, 6, 19675−19684